Raman vs Rayleigh scattering in the soft-x-ray region

Eiichi Hanamura and Hidekatsu Suzuura
Department of Applied Physics, University of Tokyo, Hongo, Bunkyo-ku, Tokyo 113, Japan

Akane Agui* and Shik Shin
Synchrotron Radiation Laboratory, Institute for Solid State Physics, University of Tokyo, Tanashi, Tokyo 188, Japan
(Received 9 April 1997)

A sharp and intense structure of the core exciton is observed in total photon yield spectra of a cubic BN crystal at 192 eV, below the transition from the boron 1*s* level to the conduction-band edge. We have discovered, however, that the Raman intensity for leaving behind the valence exciton does not show any enhancement even when the frequency of the incident field crosses the core-exciton level. This comes from the fact that relative magnitudes among the nonlinear channels depend on the relevant frequency. We analyzed the Raman spectra taking into account the strong coupling between the core exciton and radiation fields, i.e., the polariton effect, Rayleigh scattering, and the Auger process. [S0163-1829(97)09335-1]

Many similar electromagnetic phenomena have been observed over wide frequency ranges. For example, transient coherent optical effects have been successfully observed in the visible and infrared regions, while these concepts originate from the magnetic resonances in microwave frequencies. The optical laser is also a typical example, and it is an application of the maser principle to optics. The search for lasers with higher frequencies is now going on. However, it is difficult to realize ultraviolet or x-ray lasers under the present technology because spontaneous emission is too strong to be overcome by stimulated emission in such higher-frequency regions. This shows that the extension of concepts valid for the visible frequency region to x rays is highly nontrivial. Therefore, we expect that nonlinear optical responses are also dependent on the selected frequency as well as on the kind of relevant elementary excitations.

Core excitons in semiconductors and insulators have been studied theoretically[1–3] and experimentally[4–6] with a number of models and several measurement methods. Carson and Schnatterly[7] found that both the exciton intensity and binding energy could be explained with a Wannier model. Recently, synchrotron radiation sources and measurement systems have been improved to the extent that Raman scattering spectra in the soft-x-ray region,[8] and the core-exciton structure in total photon yield (TPY) spectra,[9] have been observed. These are usually interpreted by conventional extensions of concepts established in the visible frequency region.

A strong core-exciton line is observed very clearly in TPY spectra of cubic BN crystal at 192 eV, below the transition from the boron 1*s* level to the $(2sp^3)$ conduction-band edge, as shown in Fig. 1. The core exciton differs from a valence exciton in several ways. First, the core exciton has a larger binding energy than the valence exciton. The binding energy of the core exciton in cubic BN is about 2 eV. Accordingly, the oscillator strength also has a large value. Therefore, it seems that the core exciton deeply contributes to various scattering processes of electromagnetic fields. Soft-x-ray emission spectra (SXES) are also observed as a function of pump frequency, ranging from 190 eV to 195 eV, in a range about the core-exciton frequency. Observation of the Raman signal leaving behind the valance exciton is shown in Fig. 2. The valence exciton, with excitation energy 11.8 eV, is made of the conduction-band $(2sp^3)^c$ electron and the valence-band $(2sp^3)^v$ hole. This signal intensity increases very rapidly when the incident frequency ω_1 approaches the conduction-band edge excitation at the X_1 point from the boron 1*s* level. Even when, however, ω_1 crosses the

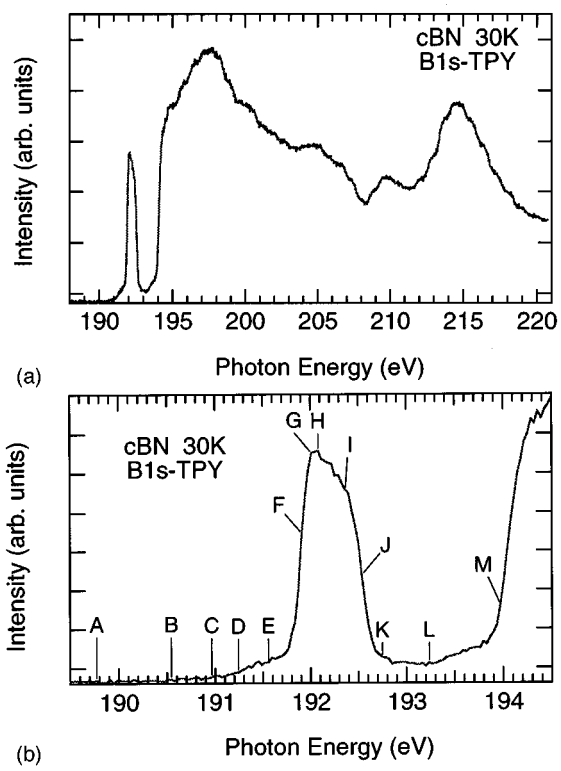

FIG. 1. (a) Total photon yield (TPY) spectrum of *c*BN at 30 K in the region of transition to the conduction-band edge from the boron 1*s* core level. (b) TPY spectrum near the core-exciton frequency, which was enlarged from part (a). $A,B,C,\ldots,M$ denote the incident frequencies at which soft-x-ray emission spectra are taken as shown in Fig. 2.

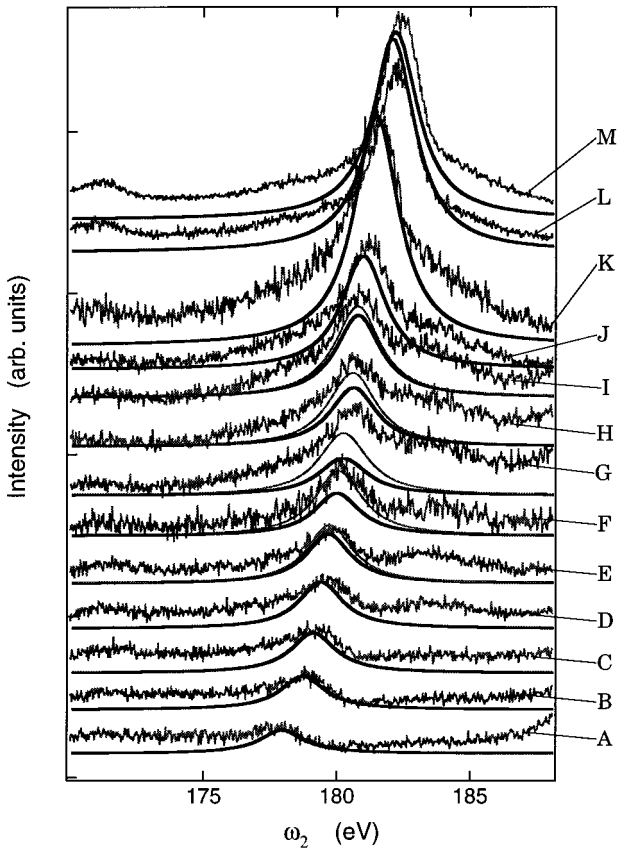

FIG. 2. Soft-x-ray emission spectra (SXES) of cBN at 30 K under excitation from the boron 1s level to just below the conduction band. $A,B,C,\ldots,N$ correspond to pump frequencies denoted in Fig. 1. Thick solid lines describe the theoretical spectra of Raman scattering leaving behind the valence exciton, and thin lines denote the calculated sum spectra of Raman scattering and luminescence.

core-exciton frequency around 192 eV, the Raman signal intensity does not increase, although this transition has a gigantic transition-dipole moment. This is in stark contrast to the case of the visible region in which Raman scattering is extremely enhanced at the exciton absorption peak. Here, it should be noted that the polariton effects become important because the core exciton has the gigantic dipole moment. What is more, it is necessary to take into account other scattering channels, i.e., Rayleigh scattering, the Auger process, etc. Although some experimental results show definite correlations between Raman and Rayleigh scattering, there have been few theoretical studies on the relation between those scattering channels. In this paper, taking these mechanisms into consideration, we have formulated the resonant Raman scattering due to the core exciton of cubic BN and analyzed the SXES, in particular, to answer the question of why the core exciton does not contribute to Raman scattering. The relative roles of Rayleigh and Raman scattering are also discussed for the first time in the soft-x-ray region.

Let us now calculate the Raman spectrum due to the core exciton. For the intermediate states created by an incident photon ω_1, the Coulomb attraction between a conduction-band electron and a hole created in the core 1s state of boron works as the intermediate state interaction and makes them form a core exciton as well as unbound electron-hole pair states. The final state created by emission of the signal photon ω_2 after absorbing the incident photon ω_1 consists of a conduction-band electron around X_1 and a hole in the valence band around X_5, and they form the valence exciton. Here the final-state interaction has also been taken into account. Then we can simplify the Hamiltonian as follows:

$$H_0=|a\rangle E_a\langle a|+\sum_b |b\rangle E_b\langle b|+|c\rangle E_c\langle c|, \tag{1}$$

$$V_0=\sum_b \{|b\rangle V_{ba}\langle a|+|c\rangle V_{cb}\langle b|+\text{H.c.}\}. \tag{2}$$

Here, H.c. denotes Hermitian conjugate terms. The initial state $|a\rangle$ consists of a ground state $|g\rangle$ of the crystal with an energy E_g and an incident photon with the frequency ω_1 created (annihilated) by $B_1^\dagger$ (B_1) so that $|a\rangle=B_1^\dagger|g\rangle$ and $E_a=E_g+\hbar\omega_1$. The final state $|c\rangle$ consists of the valence exciton and a scattered photon ω_2 created by $B_2^\dagger$. Therefore, $E_c=E_{\text{exc}}^v+\hbar\omega_2$. Here E_{exc}^v is the energy of the valence exciton. We consider many intermediate states $|b\rangle$ that are virtually and actually excited by incident photons; that is, the core-exciton state $|b_0\rangle=|n=1s,\mathbf{K}_0\rangle$, higher bound, and unbound states. Transition matrix elements between states $|a\rangle$ and $|b\rangle$ are denoted by V_{ab}. The core exciton with the wave vector $\mathbf{K}$ for the center-of-mass motion has an enhanced transition dipole moment:

$$\langle b_0|\mu|g\rangle=\sqrt{N}\mu_{\text{core}}^c f_{1s}(0)\,\delta(\mathbf{K},\mathbf{K}_0), \tag{3}$$

where μ_{core}^c is the transition-dipole moment per unit cell from the boron 1s state to the bottom X_1 of the conduction band with dominant boron 2p components, N is the total number of unit cells per unit volume, and $f_{1s}(0)$ is the envelope function at the origin $\mathbf{r}=0$ for the electron-hole relative motion in the 1s state. The electric-dipole approximation is almost satisfied, as it is electric-dipole allowed, and the size of the unit cell is still smaller than the wavelength in the soft-x-ray region. The relaxation rates of higher bound and unbound states are so large that the energy separations between the higher bound states are smeared out and therefore merge into the unbound states. As a result, the Elliott step is constituted in the absorption spectrum.[10] Note that a macroscopic enhancement of $\sqrt{N}$ is missing for the transition-dipole moment V_{bc} between a core exciton and a valence exciton and also for other transition-dipole moments.

The core-exciton state $|b_0\rangle$ is strongly coupled to the ground state $|g\rangle$ by the gigantic transition-dipole moment as stated above. Therefore, first we pick up the terms in Eqs. (1) and (2) describing the most strongly coupled levels:

$$H_0'=|a\rangle E_a\langle a|+|b_0\rangle E_{1s}^c\langle b_0|+|b_0\rangle V_0\langle a|+|a\rangle V_0\langle b_0|, \tag{4}$$

with $V_0=V_{ba}$ for $b=$ core exciton $(1s,\mathbf{K}_0)$. This is diagonalized under the following transformation:

$$\begin{pmatrix}|\alpha\rangle\\|\beta\rangle\end{pmatrix}=\begin{pmatrix}\cos\theta & \sin\theta\\ -\sin\theta & \cos\theta\end{pmatrix}\begin{pmatrix}|a\rangle\\|b_0\rangle\end{pmatrix} \tag{5}$$

and

$$H_0' = |\alpha\rangle E_\alpha \langle\alpha| + |\beta\rangle E_\beta \langle\beta| \tag{6}$$

with

$$E_{\alpha,\beta} = (\hbar\omega_1 + E_{1s}^c)/2 \pm \sqrt{(\hbar\omega_1 - E_{1s}^c)^2/4 + V_0^2}, \tag{7}$$

$$\cos\theta = V_0 / \sqrt{(E_{1s} - E_\beta)^2 + V_0^2}. \tag{8}$$

Now we define the unperturbed Hamiltonian H and interaction V as

$$H = |\alpha\rangle E_\alpha \langle\alpha| + |\beta\rangle E_\beta \langle\beta| + \sum_{b \neq b_0} |b\rangle E_b \langle b| + |c\rangle E_c \langle c|, \tag{9}$$

$$V = \sum_{b \neq b_0} [|c\rangle V_{cb} \langle b| + |b\rangle V_{ba} \{\langle\alpha|\cos\theta - \langle\beta|\sin\theta\}] + |c\rangle V_{cb_0} \{\langle\alpha|\sin\theta + \langle\beta|\cos\theta\} + \text{H.c.} \tag{10}$$

For the time being, we assume the coherence length of the exciton to cover the crystal and neglect other scattering processes, that is, relaxation effects except Raman scattering. The initial density operator $\rho_0 = |a\rangle\langle a|$ is also rewritten as

$$\rho_0 = \cos^2\theta |\alpha\rangle\langle\alpha| + \sin^2\theta |\beta\rangle\langle\beta| - \cos\theta\sin\theta \{|\alpha\rangle\langle\beta| + |\beta\rangle\langle\alpha|\}. \tag{11}$$

Off-diagonal terms can be neglected for stationary responses[11] and $\rho_0 \approx \cos^2\theta |\alpha\rangle\langle\alpha| + \sin^2\theta |\beta\rangle\langle\beta|$.

The Raman scattering spectrum $I(\omega_1, \omega_2)$, starting from the initial states $|\alpha\rangle$ and $|\beta\rangle$, is evaluated according to Refs. 11 and 12. We have the following spectrum:

$$I(\omega_1, \omega_2) = 2\pi \sum_{i=\alpha,\beta} \left| \langle c|V|i\rangle + \sum_{b \neq b_0} \frac{\langle c|V|b\rangle\langle b|V|i\rangle}{E_i - E_b} \right|^2 \times w_i \delta(E_c - E_i), \tag{12}$$

where $w_\alpha = \cos^2\theta$, $w_\beta = \sin^2\theta$ and we have set $\hbar = 1$. The energies E_i and E_c are dependent on the incident and scattered photon energies ω_1 and ω_2, respectively. This description is justified when the coherence length l_0 of the core exciton is much longer than the wavelength λ_0 of incident light ω_1. The summation over intermediate states in formula (12) does not include the core-exciton state because the initial state is a hybrid of the core exciton and the ground state with an incident photon due to the polariton effect. That is the reason why enhancement does not appear in the Raman spectra around the core-exciton resonance, while it does appear around the band-edge excitation.

As a matter of fact, the core exciton suffers from other scattering or relaxation channels, for example, Rayleigh scattering, the Auger process, dephasing relaxation (its rate is denoted by γ') and so on. Due to these processes, the core exciton decays into the ground state before Raman scattering occurs. In formula (12) for Raman scattering those other channels are well described by the decay constants as far as none of the other channels is dominant. We denote the lifetime of core excitons due to Rayleigh scattering and other channels by $T_{\text{core}} \equiv (2\gamma_c)^{-1}$. Taking account of these dephasing and lifetime effects, the eigenenergy of core exciton E_{1s}^c should be replaced by $E_{1s}^c + i\Gamma_c$, where $\Gamma_c = \gamma_c + \gamma'$. However, the splitting of E_α and E_β is not modified because of the sum rule of oscillator strength. Thus, we use the model that the coupled modes $E_{\alpha,\beta}$ suffer from the dephasing and lifetime effects proportional to their excitonic components, i.e., $E_{\alpha,\beta}$ are simply replaced by $E_{\alpha,\beta} + i\Gamma_{\alpha,\beta}$ with $\Gamma_\alpha = \Gamma_c \cos^2\theta$ and $\Gamma_\beta = \Gamma_c \sin^2\theta$. When the relaxation of valence exciton Γ_v is also taken into account, the δ-function in Eq. (12) is replaced by a Lorentzian form with half-width Γ_v. From the TPY spectrum, the $1s$ state of the core exciton is isolated and the higher bound and unbound states constitute an Elliott step. The summation over $b \neq b_0$ ($1s$ core-exciton state) corresponds to that over states composing the Elliott step. In order to compare the observed Raman spectrum with $I(\omega_1, \omega_2)$, we approximate the summation over $b \neq b_0$ by a single contribution with $E_b = E_{\text{edge}}$ (the excitation energy from the boron $1s$ level to the conduction-band edge at X_1) and introduce a parameter W for products of transition matrix elements. Then the spectrum $I(\omega_1, \omega_2)$ is simplified into the following form:

$$I(\omega_1, \omega_2) = \left\{ \left| V_0 \sin\theta + \frac{W\cos\theta}{E_\alpha(\omega_1) - E_{\text{edge}}} \right|^2 + \frac{2\gamma'}{\gamma_c} V_0^2 \sin^2\theta \right\} \frac{2\cos^2\theta(\Gamma_\alpha + \Gamma_v)}{(E_\alpha - E_{\text{exc}}^v - \omega_2)^2 + (\Gamma_\alpha + \Gamma_v)^2} + \left\{ \left| V_0 \cos\theta - \frac{W\sin\theta}{E_\beta(\omega_1) - E_{\text{edge}}} \right|^2 + \frac{2\gamma'}{\gamma_c} V_0^2 \cos^2\theta \right\} \frac{2\sin^2\theta(\Gamma_\beta + \Gamma_v)}{(E_\beta - E_{\text{exc}}^v - \omega_2)^2 + (\Gamma_\beta + \Gamma_v)^2}. \tag{13}$$

Here the luminescence components from the α and β states are also added because these channels become open only under the presence of dephasing γ'.[11] These are proportional to $2\gamma'/\gamma_c$ and the population of the excited state as given by Eq. (4.12) of the first part of Ref. 11. Now, we choose $E_{\text{edge}} = 194.75$ eV, $E_{1s}^c = 192.055$ eV, $E_{\text{exc}}^v = 11.8$ eV, $\Gamma_v = 1$ eV, and $V_0/W = 0.1\ \text{eV}^{-1}$. These numerical values, with the exception of W, are estimated from experimental data.[8,9] The value of W is only an adjustable parameter and this choice will be discussed later. The values of V_0 and Γ_c we adopted are consistent with the very small reflectance of the order of 10^{-5}–10^{-6} near the core-exciton resonance.[13] In order to evaluate $E_{\alpha,\beta}$, $\Gamma_{\alpha,\beta}$, and $\cos\theta$, we use $V_0 = 0.2$ eV, $\Gamma_c = 0.1$ eV, and $\gamma'/\gamma_c = 5$. We compare the calculated Raman spectra with the experimental results in Fig. 2 and the peak intensities of those Raman spectra are plotted in Fig. 3. An agreement between theory and experiment is excellent except at $\omega_1 \simeq E_{1s}^c$. Our theory succeeds in reproducing the experimental results, namely, that there is no enhancement in the Raman spectra due to the core exciton in spite of the sharp peak structure in TPY as shown in Fig. 1. In short, this comes from the fact that the transition dipole moment of core exciton to valence exciton is much smaller than that to the ground state; in other words, it is due to polariton effects. In addition, W comes from the summation of many intermediate states, so that the small value of $V_0/W = 0.1\ \text{eV}^{-1}$ looks reasonable.

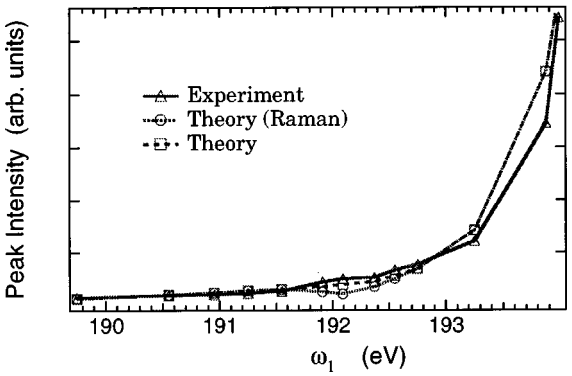

FIG. 3. The peak intensity of Raman scattering as a function of incident frequency ω_1. The solid line represents the experimental values, and dotted and dashed lines represent calculated ones for Raman scattering and for the sum of Raman scattering and luminescence, respectively.

It is worth noting that the energy splitting V_0 at the resonant excitation is not identical to the longitudinal-transverse (LT) splitting Δ_{LT}:[14]

$$V_0 \approx \sqrt{\frac{\omega_t \Delta_{\mathrm{LT}}}{2}}, \tag{14}$$

where ω_t denotes the frequency of the transverse exciton. Therefore, in the soft-x-ray region, the coupling constant V_0 between the core exciton and photon is much larger than the ordinary LT splitting Δ_{LT} because of the large $\omega_t \sim 200$ eV. It is possible that this large coupling constant V_0 gives a splitting in the Raman spectra, but the experimental spectra do not show such a clear splitting because the decay rate due to Rayleigh scattering and the Auger effect is so large. This means that Rayleigh and other scattering contributions cannot be independent of the Raman spectra and the various scattering channels are strongly correlated. The large decay rate does not break the polariton effects and the polariton splitting $2V_0$ is not modified owing to the sum rule of oscillator strength. So the formalism using the polariton concepts remains valid in this case. On the other hand, the polariton effect is negligibly small in the gas system of atoms and molecules, which was not discussed in this paper. However, Rayleigh scattering is expected to be much stronger than Raman scattering in the soft-x-ray region. The competition between these channels is one of interesting future problems in atomic or molecular gases.

We conclude that the enhancement due to the core exciton E^c_{1s} does not appear in the Raman scattering spectra leaving behind the valence exciton because the core exciton is hybridized so strongly to the ground state through its gigantic transition-dipole moment. The polariton concept survives in the soft-x-ray region. Although the polariton splitting is not clearly observed, the experimental results are well reproduced by introducing the relaxation due to Rayleigh and other scattering channels and the frequency-dependent competition between Raman and Rayleigh (and other) scattering channels is revealed.

*Present address: Department of Physics, Uppsala University, Box 530, S-751 21 Uppsala, Sweden.

[1] A. Quattropani, F. Bassani, G. Margaritondo, and G. Tinivella, Nuovo Cimento B **51**, 335 (1979).
[2] H. P. Hialmarson, M. Butner, and J. D. Dow, Phys. Rev. B **24**, 6010 (1981).
[3] A. Zunger, Phys. Rev. Lett. **50**, 1215 (1983).
[4] E. T. Arakawa and M. W. Williams, Phys. Rev. Lett. **36**, 333 (1976).
[5] F. Evangelisti, F. Patella, R. A. Riedel, G. Margaritondo, P. Fiorini, P. Perfetti, and C. Quaresima, Phys. Rev. Lett. **53**, 2504 (1984).
[6] J. F. Monar, F. J. Himpsel, G. Hollinger, G. Hughes, and J. L. Jordan, Phys. Rev. Lett. **54**, 1960 (1985).
[7] R. D. Carson and S. E. Schnatterly, Phys. Rev. Lett. **59**, 319 (1987).
[8] Y. Ma, N. Wassdahl, P. Skytt, J. Guo, J. Nordgren, P. D. Johnson, J-E. Rubensson, T. Boske, W. Eberhardt, and S. D. Kevan, Phys. Rev. Lett. **69**, 2598 (1992).
[9] S. Shin, A. Agui, M. Fujisawa, Y. Tezuka, T. Ishii, Y. Minagawa, Y. Suda, A. Ebina, O. Mishima, and K. Era, Phys. Rev. B **52**, 11 853 (1995).
[10] R. J. Elliott, Phys. Rev. **108**, 1384 (1957).
[11] T. Takagawara, E. Hanamura, and R. Kubo, J. Phys. Soc. Jpn. **43**, 802 (1977); **43**, 811 (1977); **44**, 728 (1978).
[12] Y. Toyozawa, J. Phys. Soc. Jpn. **41**, 400 (1976); A. Kotani and Y. Toyozawa, *ibid.* **41**, 1699 (1976).
[13] A. Agui and S. Shin (unpublished).
[14] J. J. Hopfield, Phys. Rev. **112**, 1555 (1958).